

From grains to powders: from single particle contact mechanics measurements to bulk powder properties

M. Kappl, L. Heim, H.-J. Butt

MPI for Polymer Research, Ackermannweg 10, 55128 Mainz, Germany

S. Luding

Particle Technology, DelftChemTech, TU Delft, Julianalaan 136, NL-2628 BL Delft, The Netherlands

R. Tykhoniuk, J. Tomas

Dept. of Mech. Process Eng., Otto-von-Guericke University of Magdeburg, Universitätsplatz 2, D - 39106 Magdeburg, Germany

ABSTRACT: Methods based on atomic force microscopy have been used to measure adhesion and sliding and rolling friction for single micron-sized particles. Model systems with low surface roughness (silica and gold particles) as well as technical products (carbonyl iron powder (CIP) particles) with less defined surface properties were used. For the model substances no significant dependence of adhesion on load was observed. For the CIP particles, plastic deformation was observed at higher loads. Comparison of the microscopic material parameters obtained for the CIP particles showed good agreement with the corresponding values obtained from Jenike shear cell experiments; this is especially true for the maximal attractive (cohesive) force. Computer simulations indicate that the macroscopic cohesion is primarily correlated to this (microscopic) maximal attractive force.

1 INTRODUCTION

To optimize the handling of fine powders in industrial applications, understanding the interaction forces between single powder particles is fundamental. With the invention of the atomic force microscope (AFM) (Binnig1986) and the introduction of the so-called “colloid probe” technique (Butt1991, Ducker1991), the direct measurement of the interaction between single micron-sized particles became possible. From such microscopic AFM measurements of the particle interaction forces it is possible to develop an appropriate contact constitutive model to describe the deformation behaviour of ultrafine, cohesive frictional particles. In this context the implementation of an irreversible inelastic contact flattening, which is an essential element and physical reason for a load-dependent increase of the adhesion force, is of vital importance. There exists a realistic and flexible microscopic model for contact laws with elastic, plastic, and adhesion forces, as based on macroscopic observations from bulk experiments (Tomas2001, Tomas2002). The model in a simplified form (Luding2003) is applied to the Jenike shear test and the biaxial shear box, in order to find out the relationship between the mechanical parameters of a single particle on a microscopic level and flow parameters of the powder “continuum” on the macroscopic level.

2 SINGLE PARTICLE MEASUREMENTS

Adhesion and friction forces were measured for single micrometer-sized particles mounted onto tipless AFM cantilever using the Particle Interaction Apparatus (PIA) and commercial AFMs as described previously (Preuss1998, Heim1999).

The adhesion between single silica spheres was found to increase linearly with the reduced radius R ($R = R_1R_2/(R_1+R_2)$ and R_1 and R_2 are the radii of the single particles) for reduced radii between 0.35 μm and 1.3 μm (Heim1999). This result shows that even for such small values of R a linear dependence between F_{adh} and R is observed, as predicted by the JKR (Johnson, Kendall and Roberts, Johnson1971) or DMT (Derjaguin, Muller and Toporov, Derjaguin1975) theories. Within the range of our experiments (maximum loads of $\approx 1 \mu\text{N}$) the adhesion force between silica particles as well as between gold particles did not depend significantly on the externally applied load.

The sliding friction of a single silica particle on a silicon wafer was found to follow a friction law $F_F = \tau A$, where F_F is the friction force, τ is the constant shear strength of the contact and A is the load dependent contact area as calculated from the JKR theory (Ecke2001). Without external load, this corresponded to a friction coefficient of 0.4.

Rolling friction between silica spheres (diameter 1.9 μm) was measured by detecting the force neces-

sary to bend chainlike agglomerates (Heim1999). The rolling friction force (defined as force acting on the center of the sphere during rolling) was found to be ~ 0.01 times the adhesion force between the spheres.

Adhesion forces between spherical carbonyl iron powder (CIP) particles were measured for reduced radii R between $0.16 \mu\text{m}$ and $1.13 \mu\text{m}$ (fig.1). The maximum applied load was 20-40 nN and contact times ranged from 0.15 to 0.40 s. Adhesion showed a tendency to increase with increasing value of R , but the scatter of the data is too large to verify the linear dependence. The large variations are mainly due to the high surface roughness of the CIP particles. The mean normalized adhesion forces F_{adh} / R had a value of $14 \pm 10 \text{ mN/m}$.

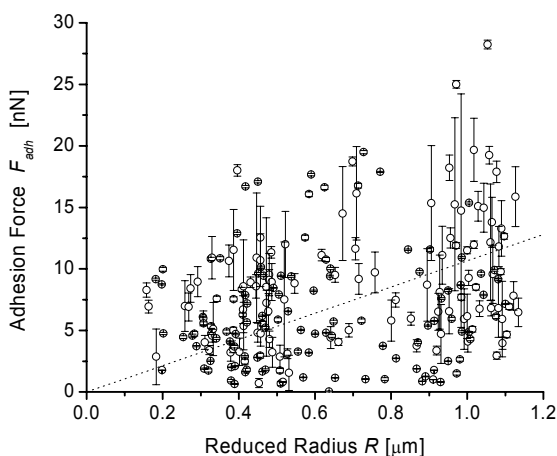


Figure 1: Dependence of the adhesion force F_{adh} between single CIP particles on the reduced radius R .

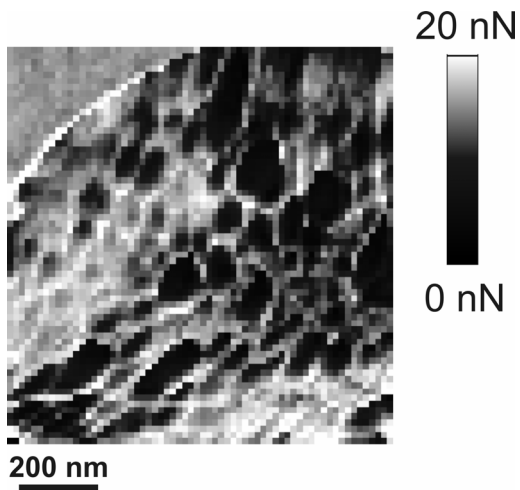


Figure 2: Spatial distribution of the adhesion force between two CIP particles.

To gain more insight in the cause for the variations, we used the so-called “Force Volume” mode (Radmacher1994, Hassan1998) that allows recording the spatial distribution of surface interactions. Figure 2 shows an example of an adhesion map that was recorded between a CIP particle glued to the substrate and a CIP particle acting as colloid probe. The region in the upper left corner consisted

of the glue used to fix the particle. Only a small variation of the adhesion force is observed on this smooth substrate. In the remaining part of the adhesion force map that corresponds to the particle-particle contact, a strong variation of the adhesion force is observed, reflecting the much higher surface roughness.

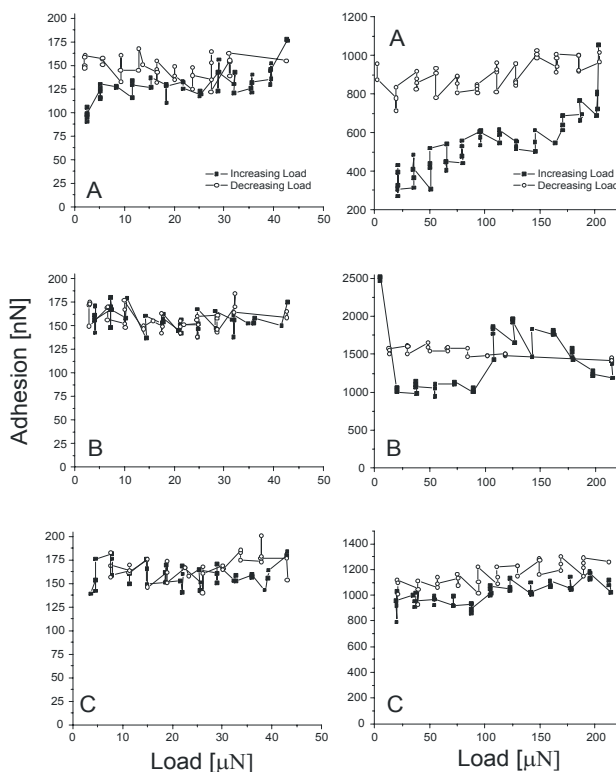


Figure 3: Load dependence of adhesion between a CIP particle and a silicon wafer for two CIP particles. See text for details.

In figure 3 the dependence of the adhesion on applied load is shown using loading forces 10^3 times higher than in fig.1. A silicon wafer was used as a reference substrate with minimum roughness. Adhesion force data for two different particles are shown. In each of the 6 plots, results for a single spot on the silicon wafer are shown where the load was first increased (full squares) and then decreased (open circles). Data in the plots “A” are from the first series of force curves with the corresponding particle, plots “B” and “C” are from consecutive series taken at other spots of the silicon wafer. Adhesion increased with load during the first cycle for both particles (about 50% for raising the load from 2.5 to 43 μN for the first and by about 160% when increasing the loading force from 21 to 204 μN for the second particle. The increased adhesion level remains upon decreasing the loading force again and stays constant in the subsequent series (plots B and C, the strong fluctuations in plot B, left may indicate a surface irregularity in this spot. This indicates plastic deformation of the contact zone. Such plastic deformation is not surprising since contact pressures can be estimated to be larger than 1 GPa and the yield stress of iron is below 350 MPa.

3 SHEAR TESTS OF COHESIVE POWDERS

Another possibility to investigate fine cohesive powders is macroscopic shear test. Results of the tests could be used for a comparison with discrete element simulations (see also parallel paper of these proceedings Tykhoniuk2005), but also can be used to “back-calculate” to a single particle values, giving qualitative information on the microscopic material parameters.

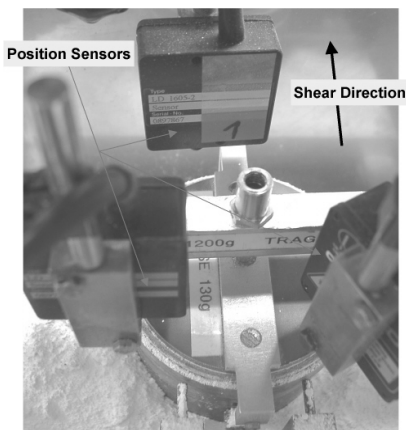


Figure 4: Translational shear cell coupled with shear lid height measurement by laser sensors

In order to compare simulations with experiments quantitatively (the shear stress values as well as the volumetric strain values), a new design of the translational shear cell involves the measurement of shear lid height and tilt (Fig. 4). The three triangulating laser displacement sensors, placed above the top of the shear cell, allow measuring the dynamic change of the shear lid height during the shear test, and thus the volumetric strain versus shear displacement.

The tests were accomplished for a limestone powder sample with the average particle diameter $d_{50} = 1.2 \mu\text{m}$, density of $\rho_s = 2740 \text{ kg/m}^3$, shear rate of $v_s = 2 \text{ mm/min}$. Fig. 5 shows an example of such tests. The powder was preconsolidated with the normal stress $\sigma_{N,0} = 16 \text{ kPa}$ and presheared with the normal stress $\sigma_{N,s} = 8 \text{ kPa}$. Normal stress during the shear procedure was taken proportional to the preshear one with the factors of 0.25, 0.4, 0.6 and 0.8. A certain compression at the beginning of the preshear process is caused by the reorganization of initial powder packing, after which the steady-state is reached. The unloading procedure (i.e. the shear drive is moved with the same rate in opposite direction, taking off in this way the force on the shear ring) causes the shear lid to settle the packing structure down to a lower porosity state again. During the load change (vertical “jumps” up and down on the figure) one can see the influence of elastic properties of a consolidated powder continuum. The reproducibility of results during the preshear is very good, and the right-hand part of the diagram shows the clear tendency: the lower is the normal stress, the higher “jumps” the shear lid.

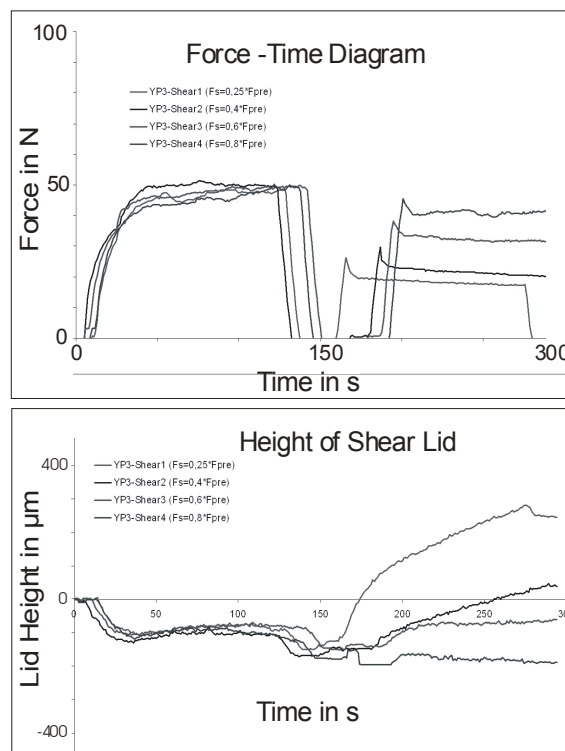


Figure 5 (Top) Shear force measurements during shear test (limestone powder); (Bottom) Volumetric strain measurements during shear test (limestone powder)

Similar measurements have been performed with the CIP powder as used in AFM measurements as well. The back calculations concerning the mean normalized adhesion force F_{adh} / R gave the result of 11.64 mN/m and showed a surprisingly good agreement with the single particle measurement values ($14 \pm 10 \text{ mN/m}$, see above).

4 NUMERICAL SIMULATIONS

For the numerical simulations of the shear tests the discrete element method (Cundall1991) was used with the contact model of Luding (Luding2005, see also parallel paper of these proceedings Tykhoniuk2005), describing the microscopic particle-particle interaction forces including a load-dependent adhesion force. Here, we use a two-dimensional bi-axial box as a model system, where the left and bottom walls are fixed. Stress- and strain-controlled deformation is applied to the side- and top-walls, respectively.

In a typical simulation, the top wall is smoothly and slowly shifted downwards, while the right wall moves, controlled by a constant stress p_x , responding on the forces exerted on it by the material in the box. Initially, the particles are randomly distributed in a huge box, with rather low overall density. Then the box is compressed by defining an external pressure, in order to achieve an isotropic initial condition with kinetic energy much smaller than the potential energy stored in the contacts. Starting from this re-

laxed, isotropic configuration, the vertical strain is applied and the response of the system is examined.

In our example $N=1950$ particles were used, with radii randomly drawn from a homogeneous distribution with minimum 0.5 mm and maximum 1.5 mm. The total mass of the particles in the system is about 0.02 kg. Without friction, the cohesion strength was varied.

From the macroscopic point of view, the flow behaviour of the system can be examined by plotting Mohr-circles for different confining pressures (left-most point on the circle) and for the maximum stress (right-most point), see Fig. 6. The tangent to these circles can be seen as the flow function for the peak stress, which corresponds to a yield locus of an overconsolidated packing. It is linear for the examined parameters with a slope larger than expected from the zero microscopic friction at the contacts.

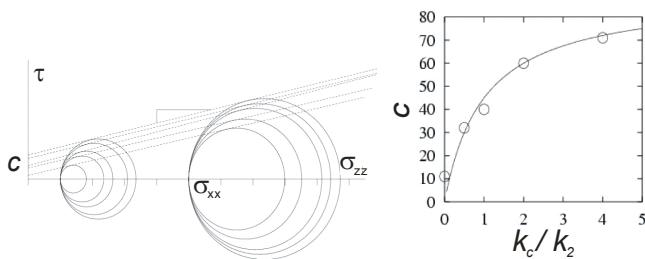


Figure 6 (Left): Mohr circle representation of the flow function at maximum stress for cohesion and no friction; (Right) Macroscopic cohesion as function of the microscopic cohesive strength. The points are taken from the flow functions, the line corresponds to the analytical expression for the maximal attractive force defined by the contact constitutive model (Luding2003, Tykhoniuk2005).

5 CONCLUSIONS

In summary, we presented experiments on single-contact measurements with an AFM based particle interaction apparatus (PIA) and extracted (besides other quantities) the magnitude of inter-particle attraction forces (about 14 mN/m). Second, from a standard Jenike shear test, the same quantity was obtained by “back-calculation” (about 12 mN/m) in reasonable quantitative agreement. As last result, the proportionality between the (microscopic) maximal attractive force, as used in DEM simulations, and the macroscopic cohesion was shown. This closes the circle for the micro-macro description, at least for the particular model materials typically used here.

In the future, the micro-macro relations for more industrially relevant materials and other material parameters have to be identified, and also the role of particle rotations is an open issue, as related to micro-polar constitutive models. Further studies in the same spirit are currently in progress, involving AFM measurements, shear-test experiments, and three-dimensional DEM simulations.

6 ACKNOWLEDGEMENTS

The authors acknowledge the financial support from the German Research Foundation (DFG).

REFERENCES

- Binnig, G. et al. 1986 Atomic force microscope. *Phys. Rev. Lett.* 56: 930-933.
- Butt, H.-J. 1991. Measuring electrostatic, van der Waals, and hydration forces in electrolyte solutions with an atomic force microscope. *Biophys. J.* 60: 1438-1444.
- Cundall, P. A & Hart, R. D. 1992. Numerical modelling of diskontinua. 1st US Conference on DEM. *Eng. Comput.* 9, 101-113.
- Derjaguin, B.V. et al. 1975. Effect of contact deformations on the adhesion of particles. *J. Colloid Interface Sci.* 53:314-326.
- Ducker, W.A. et al. 1991. Direct measurement of colloidal forces using an atomic force microscope. *Nature* 353: 239-241.
- Hassan, E. 1998. Relative Microelastic Mapping of Living Cells by Atomic Force Microscopy. *Biophys. J.* 74: 1564-1578.
- Heim, L.O. et al. 1999. Adhesion and friction forces between spherical micrometer-sized particles. *Phys. Rev. Lett.* 83: 3328-3331.
- Larsen, R.I. 1958. The adhesion and removal of particles attached to air filter surfaces. *Am. Indust. Hyg. J.* 19: 265 – 270.
- Israelachvili, J.N. & Tabor, D. 1972. The measurement of van der Waals dispersion forces in the range of 1.5 to 130 nm. *Proc. R. Soc. Lond. A* 331: 19-38.
- Johnson, K.L. et al. 1971. Surface energy and contact of elastic solids, *Proc. Royal Soc. London A.* 324: 301-313.
- Luding, S., Tykhoniuk, R. & Tomas, J. 2003. Anisotropic material behaviour in dense, cohesive powders. *Chem. Eng. Tech.* 26 (12), 1229-1232.
- Luding, S. 2005. Shear flow modeling of cohesive and frictional fine powder. *Powder Technology* submitted
- Podcheck, F. & Newton, J.M. 1995. Adhesion and friction between powders and polymer or aluminum surfaces determined by a centrifuge technique, *J. Pharmaceutical Sci.* 84: 1067-1071.
- Polke, R. 1969 Adhesion of solids at elevated temperatures, *Bull. Soc. Special Chim. France* A3241: 51-54
- Preuss, M. & Butt, H.-J. 1998. Measuring the contact angle of individual colloidal particles. *J. Colloid Interface Sci.* 208: 468-477.
- Radmacher, M. et al. 1994. Mapping interaction forces with the atomic force microscope, *Biophys. J.* 66: 2159-2165.
- Tabor, D. & Winterton, R.H.S. 1968. Surface forces: direct measurement of normal and retarded van der Waals forces. *Nature* 219: 1120-1121.
- Tomas, J. 2001. Assessment of mechanical properties of cohesive particulate solids – part 1: particle contact constitutive model. *Particulate Science & Technology* 19-2, 95-110.
- Tomas, J. 2002. Zur Mechanik trockener kohäsiver Schüttgüter. *Schüttgut* 8-6, 522-537.
- Tykhoniuk, R., Tomas, J., Luding, S., Kappl, M., Heim, L., & Butt, H.-J. 2005. Adhesion, Inelastic Contact Behaviour and Simulation of Shear Dynamics of Ultrafine Cohesive Powder, *Proc. of Powders&Grains 2005*.